APR 2 1 2006

REPORT DOCUMENTATION PAGE	Form Approved OMB No. 0704-0188

1. AGENCY USE ONLY *(Leave blank)*	2. REPORT DATE	3. REPORT TYPE AND DATES COVERED
	14.Apr.06	MAJOR REPORT

4. TITLE AND SUBTITLE
MODIFIED GENERALIZED-ALPHA METHOD FOR INTEGRATING GOVERNING EQUATIONS OF VERY FLEXIBLE AIRCRAFT.

5. FUNDING NUMBERS

6. AUTHOR(S)
MAJ SHEARER CHRISTOPHER M

7. PERFORMING ORGANIZATION NAME(S) AND ADDRESS(ES)
UNIVERSITY OF MICHIGAN

8. PERFORMING ORGANIZATION REPORT NUMBER
CI04-1764

9. SPONSORING/MONITORING AGENCY NAME(S) AND ADDRESS(ES)
THE DEPARTMENT OF THE AIR FORCE
AFIT/CIA, BLDG 125
2950 P STREET
WPAFB OH 45433

10. SPONSORING/MONITORING AGENCY REPORT NUMBER

11. SUPPLEMENTARY NOTES

12a. DISTRIBUTION AVAILABILITY STATEMENT
Unlimited distribution
In Accordance With AFI 35-205/AFIT Sup 1

12b. DISTRIBUTION CODE

13. ABSTRACT *(Maximum 200 words)*

DISTRIBUTION STATEMENT A
Approved for Public Release
Distribution Unlimited

14. SUBJECT TERMS

15. NUMBER OF PAGES
20

16. PRICE CODE

17. SECURITY CLASSIFICATION OF REPORT	18. SECURITY CLASSIFICATION OF THIS PAGE	19. SECURITY CLASSIFICATION OF ABSTRACT	20. LIMITATION OF ABSTRACT

THE VIEWS EXPRESSED IN THIS ARTICLE ARE THOSE OF THE AUTHOR AND DO NOT REFLECT THE OFFICIAL POLICY OR POSITION OF THE UNITED STATES AIR FORCE, DEPARTMENT OF DEFENSE, OR THE U.S. GOVERNMENT.

Modified Generalized-α Method for Integrating Governing Equations of Very Flexible Aircraft

Christopher M. Shearer * and Carlos E. S. Cesnik †
The University of Michigan, Ann Arbor, Michigan, 48109, USA

I. Abstract

This paper focuses on the time integration of the nonlinear EOM associated with a very flexible aircraft in flight. Various integration methods exist for linear structural dynamics problems. However, a review of the literature indicates little material associated with the integration of nonlinear structural EOM of relatively large order. Moreover, for the problem of simulation of very flexible aircraft, a combination of flight dynamics and aeroelastic degrees of freedom must be integrated concurrently. A modified first and second order Generalized-α Method along with an implicit sub-iteration scheme were developed. It has shown good agreement with predictor/corrector integration schemes for a reduced set of linear EOM. The method is also seen to be numerically stable when compared to non-dissipative time marching integration schemes and requires less computational time compared to predictor/corrector methods for the full set of nonlinear EOM.

II. Introduction

Recent advances in airborne sensors and communication packages have brought the need for high-altitude long-endurance (HALE) aircraft. These platforms can be categorized under three broad missions supporting either the military or civilian community. The missions include airborne Intelligence, Surveillance, and Reconnaissance (ISR) for the military,[1] network communication nodes for the military and civilian community,[2] and general atmospheric research.[2] Due to the mission requirements, the desired vehicles are characterized by high aspect ratio wings and slender fuselages. Example of mission optimization studies for this class of vehicle can be found in Ref. 1 where the authors show that the HALE aircraft are required to have a fuel fraction greater than 66%, resulting in a very small structural weight fraction. Therefore, the combination of high aerodynamic efficiency and low structural weight fraction results in inherently very flexible vehicles. The HALE vehicle may then present large dynamic wing deformations at low frequencies, presenting a direct impact into the flight dynamic characteristics of the vehicle.

In the process of developing and subsequently integrating the resulting set of nonlinear second- and first-order differential equations,[3] an adaptation of the Generalized-α Method[4,5] was developed by the authors. The resulting set of second-order nonlinear elastic equations of motion (EOM) and the first-order body EOM are coupled with Peters[6,7] finite state inflow model. The resulting set of second- and first-order differential equations are then integrated using a modified implicit Generalized-α Method. The Generalized-α Method is a time marching high-frequency dissipative integration scheme developed for linear systems. When integrating structural dynamical problems, frequently the need arises for a dissipative method to prevent high frequency numerical errors from accumulating and affecting the low frequency dynamics of interest.

The high-frequency errors are due to the integration of a set of stiff set of equations.[8,9] Stiff systems are defined as one with a large condition number (ratio of the largest singular value divided by the smallest) or a system with a very wide spread of time constants.[10] The resulting set of differential equations[3] are

*Major, USAF, PhD Candidate, Student Member, shearerc@umich.edu.
†Associate Professor of Aerospace Engineering, AIAA Associate Fellow, cesnik@umich.edu.

inherently stiff. Additionally the equations can be augmented with constraint algebraic equations to impose relative or absolute motion constraints.

A. Previous Work

Several authors have expanded the field of structural dynamics time marching integration schemes. Newmark[11] was one of the earliest researchers who saw the need for dissipative numerical integration schemes for structural dynamics. That work was followed, among others, by Hilber, Hughes, and Taylor[12] (HHT) who extended the Newmark method. Several other authors contributed to the body of knowledge are summarized by Fung's review of time marching algorithms using numerical dissipation.[13]

Several of the time marching dissipative methods were then brought together in a single second order formulation by Chung and Hulbert.[4] This formulation incorporates the Newmark, HHT, Wilson-θ, and trapezodial methods. Seeing the need for a first-order high-frequency dissipative method, Jansen, Whiting, and Hulbert[5] extended the second-order method to a first-order one originally for the integration of computational fluid dynamics equations. Supporting the use of numerically dissipative integration schemes, Cardona and Geradin[8] proved the importance of using these schemes for the integration of constrained EOM with finite rotations.

Alternate methods of dealing with numerical instability associated with stiff system of equations have been developed by several researchers.[9,14–17] These researchers have developed various momentum and energy preserving schemes as well as momentum preserving and energy decaying schemes. These methods typically have slightly better convergence properties than the Generalized-α Method. All the methods have been shown to work well with conservative or state independent generalized forces. Zhou and Tamma[18] have developed a more general single step integration scheme for linear structural dynamics problems incorporating numerical dissipation. Kane and Levison[19,20] and Sochet[21] extended the integration schemes by developing various checking functions used to post process a numerical integration and determine its error.

Panda[22] presented the highlights of a Newton-Raphson sub-iteration technique which utilized the parent Newmark-β time integration scheme for second-order EOM developed for flexible rotorcraft problems. The main difference between Panda's[22] formulation and the method presented here is the incorporation of first-order differential equations. Additional differences with respect to his paper are the use of the Generalized-α time marching integration scheme, a generic beam model formulation, detailed implementation schemes, and comparative results.

Researchers studying nonlinear aeroelastic effects have used a variety of techniques. Patil and Hodges 2005 IFASD, utilized a second-order, central-difference, time marching algorithm with high frequency damping, page 14. Drela[23] uses a second order backward difference method, with a sub-iteration step in his ASWING code. Tang and Dowell[24,25] used a reduced order model and a Runge-Kutta integration scheme. Patil, et. al.[26,27] utilized a time-marching scheme based upon space-time finite elements. Brown[28] and Cesnik and Brown[29] utilized a trapezoidal integration scheme for flexible and limited rigid body motions. These various methods have shown difficulty in integrating the EOM developed by Shearer and Cesnik[3] either through numerical instability or severely increased computational burden.

The Generalized-α Method was selected based upon its relative ease of implementation with the current EOM modeling and the availability of both first- and second-order formulations.[4,5] The two methods are modified using an implicit integration scheme detailed by Geradin and Rixen[30] for nonlinear second-order EOM. The second-order Generalized-α Method is used to integrate the flexible EOM, while the first-order method is used to integrate the body EOM and remaining differential equations developed by Shearer and Cesnik.[3] The use of second- and first-order integration schemes keep the size of the resulting sub-iteration tangent matrices significantly smaller than if the second-order equations were transformed to a set of first-order differential equations.

B. Objective of the paper

The objective of this paper is to present an implicit time marching numerical integration method for use with coupled first- and second-order nonlinear differential equations of motion, termed the Modified Generalized-α Method. The proposed method addresses long term integration stability and computational performance for a large nonlinear elastic system.

III. Theoretical Development

The theoretical development is comprised of four sub-sections. The first section is a review of the Generalized-α Method for first- and second-order linear systems. The second section presents a summary of the particular first- and second-order EOM to be solved. The third section reviews and extends Geradin and Rixen's [30] method for nonlinear systems using a dissipative time marching integration scheme and provides the details for the very flexible aircraft EOM. The final section presents the details of the convergence criteria required for each time step.

A. Review of the Generalized-α Method

The Generalized-α Method[4] is designed to solve the second order linear differential equation of the form

$$M\mathbf{a} + C\mathbf{v} + K\mathbf{d} = \mathbf{F} \tag{1}$$

where M, C, and K are generalized mass, damping and stiffness matrices, $\mathbf{a}$, $\mathbf{v}$, and $\mathbf{d}$ are generalized acceleration, velocity, and displacement, and $\mathbf{F}$ is the generalized force vector. The Generalized-α Method then solves for the a discrete time step, n, using

$$\mathbf{d}_{n+1} = \mathbf{d}_n + h\mathbf{v}_n + h^2\left(\left(\frac{1}{2} - \beta_2\right)\mathbf{a}_n + \beta_2\mathbf{a}_{n+1}\right) \tag{2}$$

$$\mathbf{v}_{n+1} = \mathbf{v}_n + h\left((1-\gamma_2)\,\mathbf{a}_n + \gamma_2\mathbf{a}_{n+1}\right) \tag{3}$$

$$\mathbf{F}\left(t_{n+1-\alpha_{f_2}}\right) = M\mathbf{a}_{n+1-\alpha_{m_2}} + C\mathbf{v}_{n+1-\alpha_{f_2}} + K\mathbf{d}_{n+1-\alpha_{f_2}} \tag{4}$$

where h is the time step defined by

$$h = t_{n+1} - t_n \tag{5}$$

and

$$\mathbf{d}_{n+1-\alpha_{f_2}} = (1-\alpha_{f_2})\,\mathbf{d}_{n+1} + \alpha_{f_2}\mathbf{d}_n \tag{6}$$

$$\mathbf{v}_{n+1-\alpha_{f_2}} = (1-\alpha_{f_2})\,\mathbf{v}_{n+1} + \alpha_{f_2}\mathbf{v}_n \tag{7}$$

$$\mathbf{a}_{n+1-\alpha_{m_2}} = (1-\alpha_{m_2})\,\mathbf{a}_{n+1} + \alpha_{m_2}\mathbf{a}_n \tag{8}$$

$$t_{n+1-\alpha_{f_2}} = (1-\alpha_{f_2})\,t_{n+1} + \alpha_{f_2}t_n \tag{9}$$

The parameters α_{f_2}, α_{m_2}, γ_2, and β_2 are used to control the amplification of high frequency numerical modes which are not of interest. If the parameters are chosen correctly, HHT, Newmark or WBZ methods can be recovered. However, for this study the following relationships are used

$$\gamma_2 = \frac{1}{2} - \alpha_{m_2} + \alpha_{f_2} \tag{10}$$

$$\beta_2 = \frac{1}{4}\left(1 - \alpha_{m_2} + \alpha_{f_2}\right)^2 \tag{11}$$

$$\alpha_{m_2} = \frac{2\rho_{\infty_2} - 1}{\rho_{\infty_2} + 1} \tag{12}$$

$$\alpha_{f_2} = \frac{\rho_{\infty_2}}{\rho_{\infty_2} + 1} \tag{13}$$

where the subscript 2 refers to the second-order system, Eq. 1, and will be necessary to distinguish γ_2, α_{m_2}, and α_{f_2} values from the first-order EOM counterpart. The single parameter ρ_{∞_2} is used to control the numerical dissipation above the normalized frequency h/T, where T is the period associated with the highest frequency of interest and

$$0 \leq \rho_\infty \leq 1 \tag{14}$$

If ρ_∞ is chosen to be unity then the trapezoidal method is recovered. If ρ_∞ is chosen to be 0 then frequencies above h/T will be dissipated in one time step, a so called "asymptotic annihilation."

In a similar manner Jansen, Whiting and Hulbert[5] developed the first-order Generalized-α Method for a first-order system of the form

$$\dot{x} = ax \tag{15}$$

where the following relationships are employed

$$\dot{x}_{n+\alpha_{m_1}} = a x_{n+\alpha_{f_1}} \tag{16}$$
$$x_{n+1} = x_n + h\dot{x}_n + h\gamma_1 \left(\dot{x}_{n+1} - \dot{x}_n\right) \tag{17}$$
$$\dot{x}_{n+\alpha_{m_1}} = \dot{x}_n + \alpha_{m_1} \left(\dot{x}_{n+1} - \dot{x}_n\right) \tag{18}$$
$$x_{n+\alpha_{f_1}} = x_n + \alpha_{f_1} \left(x_{n+1} - x_n\right) \tag{19}$$

In a similar manner to the second-order Generalized-α Method the free parameters γ_1, α_{m_1}, and α_{f_1} can be chosen in terms of a single high frequency spectral radius parameter, ρ_{∞_1}, by

$$\gamma_1 = \frac{1}{2} + \alpha_{m_1} - \alpha_{f_1} \tag{20}$$
$$\alpha_{m_1} = \frac{1}{2}\left(\frac{3 - \rho_{\infty_1}}{1 + \rho_{\infty_1}}\right) \tag{21}$$
$$\alpha_{f_1} = \frac{1}{1 + \rho_{\infty_1}} \tag{22}$$

B. Differential Equations for a Very Flexible Aircraft

The nonlinear equations of motion for a very flexible aircraft have been presented in Shearer and Cesnik.[3] An orthogonal reference frame B is placed at point O, which in general is not the center of mass of the vehicle, as shown in Figure 1. The resulting set of differential equations can be summarized as

$$M_{FF}\ddot{\epsilon} = -M_{FB}\dot{\beta} - C_{FF}\dot{\epsilon} - C_{FB}\beta - K_{FF}\epsilon + R_F \tag{23}$$
$$M_{BB}\dot{\beta} = -M_{BF}\ddot{\epsilon} - C_{BB}\beta - C_{BF}\dot{\epsilon} + R_B \tag{24}$$
$$\dot{\zeta} = -\frac{1}{2}\Omega_\zeta \zeta \tag{25}$$
$$\dot{p}_B = \begin{bmatrix} C^{GB} & 0 \end{bmatrix} \beta \tag{26}$$
$$\dot{\lambda} = F_1 \begin{Bmatrix} \ddot{\epsilon} \\ \dot{\beta} \end{Bmatrix} + F_2 \begin{Bmatrix} \dot{\epsilon} \\ \beta \end{Bmatrix} + F_3 \lambda \tag{27}$$

where Eq. 23 is the governing nonlinear structural second order EOM, Eq. 24 is the B reference frame first order nonlinear EOM, Eq. 25 is the propagation of the orientation of the B reference frame using quaternion parameters,[10] Eqs. 26 and 27 represents the unsteady aerodynamic effects through induced inflow over the lifting surfaces. The variables are defined as

$\epsilon \equiv$ strain vector
$\beta \equiv$ vector of translational and rotational velocities
$\zeta \equiv$ quaternion parameters for B reference frame orientation
$p_B \equiv$ vector components of B reference frame location
$\lambda \equiv$ unsteady inflow velocities

Three possible solutions to Eqs. 23-27 are given in Shearer and Cesnik.[3] First, by reducing the order of the equations by eliminating all elastic DOF, a simple rigid body solution emerged. Second is a linearized solution, where the generalized mass matrix is only a function of the initial state. Third is a full nonlinear simulation where the generalized mass matrix is updated at each time step. The matrices of Eqs. 23-27 are functions of the states, ϵ, β, ζ, λ as

$$\begin{aligned} M_{FF}, M_{FB}, M_{BF}, M_{BB} &= f(\epsilon) \\ C_{FF}, C_{BF} &= f(\epsilon, \dot{\epsilon}) \\ C_{FB}, C_{BB} &= f(\epsilon, \dot{\epsilon}, \beta) \\ \Omega_\zeta &= f(\beta) \\ C^{GB} &= f(\zeta) \end{aligned} \tag{28}$$

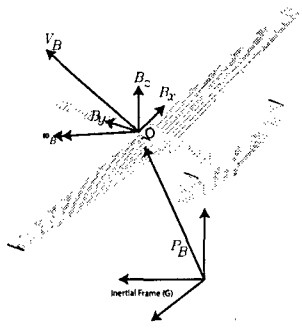

Figure 1. Basic Body Reference Frame and Vehicle Coordinates

C. Implicit Integration Scheme Utilizing Generalized-α Method

The Generalized-α Method was designed for linear systems but is implemented here in solving a non-linear problem. In general all numerical integration schemes follow the flow given in Figure 2. The differences between integration schemes are imbedded in the "Subiteration Routine" block. For a trapezodial method, this block consists of the amplification matrix, A, which solves

$$x_{n+1} = [A]\, x_n \tag{29}$$

where n is a discrete time step and x are the system states. In the modified Generalized-α Method the basic concept at each time step is to predict the states and their time derivatives and employ a sub-iteration Newton-Raphson method to correct the state predictions. The sub-iteration is repeated until a user defined tolerance is met. The implicit integration scheme chosen resembles Geradin's and Rixen's method[30] and the flow is shown in Figure 3. The specific convergence flow is shown in Figure 4.

1. Predictors

To begin the sub-iteration loop, Figure 3, the states at time step $n+1$ are predicted. For the second order EOM, Geradin and Rixen[30] provide a set of predictors q^*_{n+1}, $\dot{q}^*_{n+1}$, and $\ddot{q}^*_{n+1}$ given the states at the current time step, n, q_n, $\dot{q}_n$, and $\ddot{q}_n$ as

$$q^*_{n+1} = q_n + h\dot{q}_n + \left(\frac{1}{2} - \beta_2\right) h^2 \ddot{q}_n \tag{30}$$

$$\dot{q}^*_{n+1} = \dot{q}_n + (1 - \gamma_2)\, h\ddot{q}_n \tag{31}$$

$$\ddot{q}^*_{n+1} = 0 \tag{32}$$

In a similar manner to Geradin and Rixen,[30] the first order EOM predictors, x^*_{n+1} and $\dot{x}^*_{n+1}$ are proposed as

$$x^*_{n+1} = x_n + h\,(1 - \gamma_1)\,\dot{x}_n \tag{33}$$

$$\dot{x}^*_{n+1} = 0 \tag{34}$$

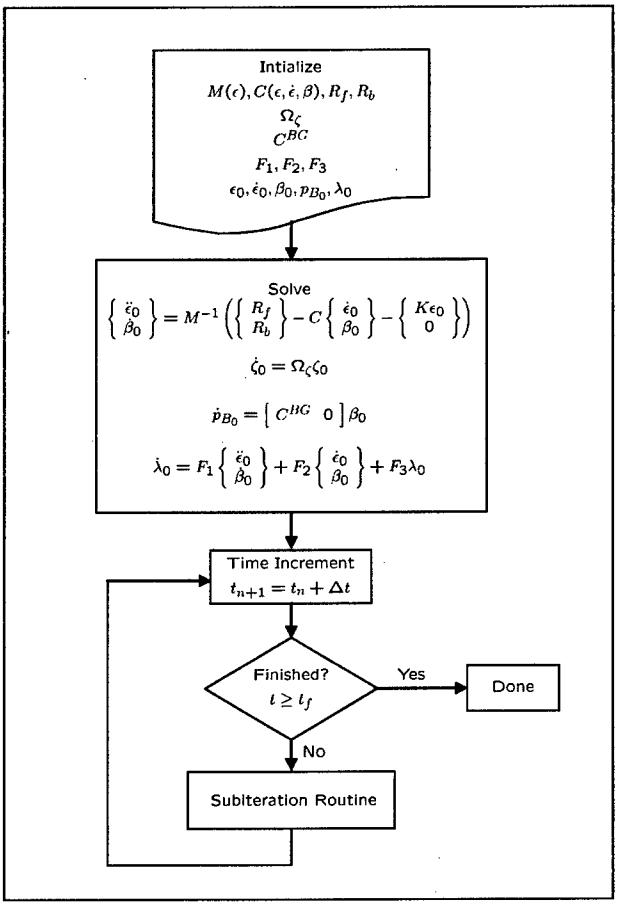

Figure 2. Basic Numerical Integration Flow

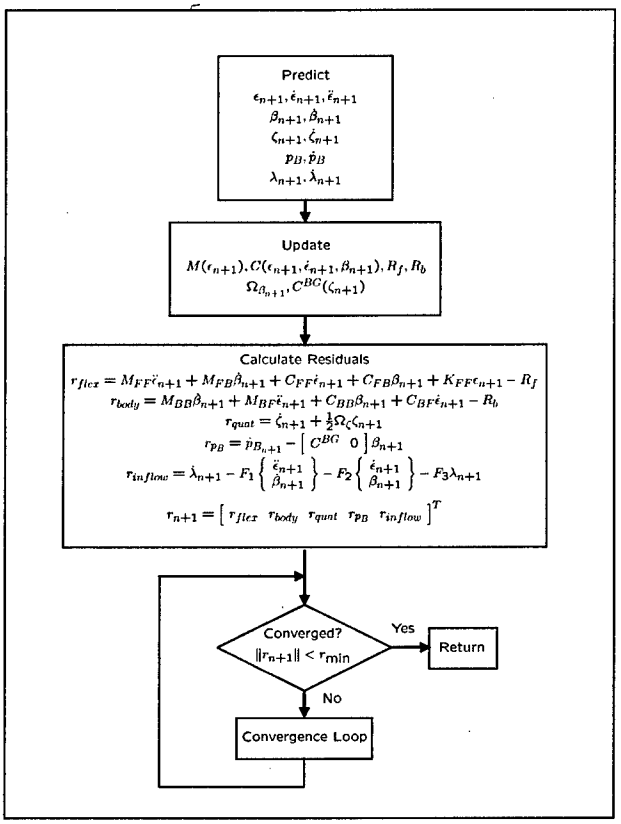

Figure 3. Sub-iteration Routine

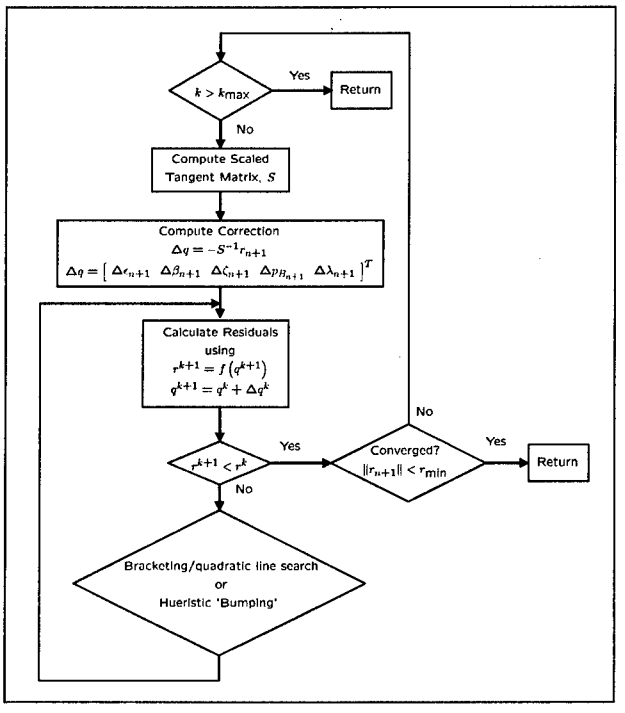

Figure 4. Sub-iteration Convergence Flow

2. Newton-Raphson: Residual Terms and the Tangent Matrix

The predictors of Eqs. 30-34 are substituted back into the governing differential equations, Eqs 23-27, where all the terms are moved to the left side. The result is a set of residual terms, r, defined as

$$r_f = M_{FF}\ddot{\epsilon} + M_{FB}\dot{\beta} + C_{FF}\dot{\epsilon} + C_{FB}\beta + K_{FF}\epsilon - R_F \tag{35}$$

$$r_b = M_{BB}\dot{\beta} + M_{BF}\ddot{\epsilon} + C_{BB}\beta + C_{BF}\dot{\epsilon} - R_B \tag{36}$$

$$r_q = \dot{\zeta} + \frac{1}{2}\Omega_\zeta \zeta \tag{37}$$

$$r_p = \dot{p}_B - \left[\begin{array}{cc} C^{GB} & 0 \end{array}\right]\beta \tag{38}$$

$$r_i = \dot{\lambda} - F_1 \left\{\begin{array}{c} \ddot{\epsilon} \\ \dot{\beta} \end{array}\right\} - F_2 \left\{\begin{array}{c} \dot{\epsilon} \\ \beta \end{array}\right\} - F_3\lambda \tag{39}$$

where

$$r = \left[\begin{array}{ccccc} r_f & r_b & r_q & r_p & r_i \end{array}\right]^T \tag{40}$$

A Taylor series expansion of the residual vector, r_{n+1}^{k+1}, at time step $n+1$ and sub-iteration step $k+1$ yields

$$r_{n+1}^{k+1} = r_{n+1}^{k} + \left[\frac{\partial}{\partial q} r_{n+1}^{k}\right]\left(q_{n+1}^{k+1} - q_{n+1}^{k}\right) + \mathcal{H}.\mathcal{O}.\mathcal{T}. \tag{41}$$

and

$$q = \left[\begin{array}{ccccc} \epsilon^T & \beta^T & \zeta^T & p_B^T & \lambda^T \end{array}\right]^T \tag{42}$$

Setting the higher order terms to zero, assuming $r_{n+1}^{k+1} = 0$, and defining the tangent matrix S_{n+1}^{k}

$$S_{n+1}^{k} = \left[\frac{\partial}{\partial \Delta q^k} r_{n+1}^{k}\right] \tag{43}$$

where

$$\Delta q^k = q_{n+1}^{k+1} - q_{n+1}^k \tag{44}$$

Δq^k is solved as

$$\Delta q^k = -\left[S_{n+1}^k\right]^{-1} r_{n+1}^k \tag{45}$$

Here Δq^k can be the correction term for either a first or second order differential equation depending upon the structure of the tangent matrix. For the governing differential equations, Eqs. 23-27, the full tangent matrix takes the form

$$S_{n+1}^k = \begin{bmatrix} \left[\frac{\partial}{\partial \Delta \epsilon^k}(r_f)_{n+1}^k\right] & \left[\frac{\partial}{\partial \Delta \beta^k}(r_f)_{n+1}^k\right] & \left[\frac{\partial}{\partial \Delta \zeta^k}(r_f)_{n+1}^k\right] & \left[\frac{\partial}{\partial \Delta p_B^k}(r_f)_{n+1}^k\right] & \left[\frac{\partial}{\partial \Delta \lambda^k}(r_f)_{n+1}^k\right] \\ \left[\frac{\partial}{\partial \Delta \epsilon^k}(r_b)_{n+1}^k\right] & \left[\frac{\partial}{\partial \Delta \beta^k}(r_b)_{n+1}^k\right] & \left[\frac{\partial}{\partial \Delta \zeta^k}(r_b)_{n+1}^k\right] & \left[\frac{\partial}{\partial \Delta p_B^k}(r_b)_{n+1}^k\right] & \left[\frac{\partial}{\partial \Delta \lambda^k}(r_b)_{n+1}^k\right] \\ \left[\frac{\partial}{\partial \Delta \epsilon^k}(r_q)_{n+1}^k\right] & \left[\frac{\partial}{\partial \Delta \beta^k}(r_q)_{n+1}^k\right] & \left[\frac{\partial}{\partial \Delta \zeta^k}(r_q)_{n+1}^k\right] & \left[\frac{\partial}{\partial \Delta p_B^k}(r_q)_{n+1}^k\right] & \left[\frac{\partial}{\partial \Delta \lambda^k}(r_q)_{n+1}^k\right] \\ \left[\frac{\partial}{\partial \Delta \epsilon^k}(r_p)_{n+1}^k\right] & \left[\frac{\partial}{\partial \Delta \beta^k}(r_p)_{n+1}^k\right] & \left[\frac{\partial}{\partial \Delta \zeta^k}(r_p)_{n+1}^k\right] & \left[\frac{\partial}{\partial \Delta p_B^k}(r_p)_{n+1}^k\right] & \left[\frac{\partial}{\partial \Delta \lambda^k}(r_p)_{n+1}^k\right] \\ \left[\frac{\partial}{\partial \Delta \epsilon^k}(r_i)_{n+1}^k\right] & \left[\frac{\partial}{\partial \Delta \beta^k}(r_i)_{n+1}^k\right] & \left[\frac{\partial}{\partial \Delta \zeta^k}(r_i)_{n+1}^k\right] & \left[\frac{\partial}{\partial \Delta p_B^k}(r_i)_{n+1}^k\right] & \left[\frac{\partial}{\partial \Delta \lambda^k}(r_i)_{n+1}^k\right] \end{bmatrix} \tag{46}$$

The tangent matrix S_{n+1}^k given by Eq. 46 in practice tends to have a large condition number due to the stiffness of the governing differential equations. This creates a problem with numerical accuracy when inverting S_{n+1}^k. In order to reduce the condition number and improve numerical accuracy, the tangent matrix is scaled with the scalar quantities d_j according to

$$\hat{S}_{n+1_{ij}}^k = S_{n+1_{ij}}^k \cdot d_j \tag{47}$$

The scalar values, d_j, are found so to minimize the condition number of $\hat{S}_{n+1}^k$. Equation 45 is then modified as

$$\begin{aligned} \Delta \hat{q}^k &= -\left[\hat{S}_{n+1}^k\right]^{-1} r_{n+1}^k \\ \Delta q^k &= \begin{bmatrix} d_1 \Delta \hat{q}_1^k & d_2 \Delta \hat{q}_2^k & \cdots & d_5 \Delta \hat{q}_5^k \end{bmatrix}^T \end{aligned} \tag{48}$$

3. Correction Terms

For second order differential equations the states and their derivatives are updated as[30]

$$\begin{aligned} q_{n+1}^{k+1} &= q_{n+1}^k + \Delta q^k \\ \dot{q}_{n+1}^{k+1} &= \dot{q}_{n+1}^k + \left(\frac{\gamma_2}{\beta_2 h}\right) \Delta q^k \\ \ddot{q}_{n+1}^{k+1} &= \ddot{q}_{n+1}^k + \left(\frac{1}{\beta_2 h^2}\right) \Delta q^k \end{aligned} \tag{49}$$

For the first order differential, equations the updated states and the first derivative terms are found to be

$$\begin{aligned} q_{n+1}^{k+1} &= q_{n+1}^k + \Delta q^k \\ \dot{q}_{n+1}^{k+1} &= \dot{q}_{n+1}^k + \left(\frac{1}{\gamma_1 h}\right) \Delta q^k \end{aligned} \tag{50}$$

This is derived starting with the update equation of q_{n+1}, Ref. 5, Eq. 13

$$q_{n+1} = q_n + h\dot{q}_n + h\gamma_1 \left(\dot{q}_{n+1} - \dot{q}_n\right) \tag{51}$$

where the following substitutions were made

$$q = y, \qquad h = \Delta t, \qquad \gamma_1 = \gamma \tag{52}$$

Equation 51 can be solved for $\dot{q}_{n+1}$ as

$$\dot{q}_{n+1} = \frac{1}{\gamma_1 h}\left(q_{n+1} - \left(q_n + h\left(1-\gamma_1\right)\dot{q}_n\right)\right) \tag{53}$$

Substituting Eq. 33 into Eq. 53

$$\dot{q}_{n+1} = \frac{1}{\gamma_1 h}\left(q_{n+1} - q^*_{n+1}\right) \tag{54}$$

and defining

$$\Delta q = q_{n+1} - q^*_{n+1} \tag{55}$$

Eq. 50 is recovered. Using Eqs. 49 and 50 the partial derivatives of the states and their derivatives with respect to Δq can now be computed. For second order differential equations the derivatives are

$$\begin{aligned}\left[\frac{\partial}{\partial \Delta q}\ddot{q}\right] &= \frac{1}{\beta_2 h^2} \\ \left[\frac{\partial}{\partial \Delta q}\dot{q}\right] &= \frac{\gamma_2}{\beta_2 h} \\ \left[\frac{\partial}{\partial \Delta q} q\right] &= 1\end{aligned} \tag{56}$$

(57)

and for first order

$$\left[\frac{\partial}{\partial \Delta q}\dot{q}\right] = \frac{1}{\gamma_1 h} \tag{58}$$

$$\left[\frac{\partial}{\partial \Delta q} q\right] = 1 \tag{59}$$

Using Eqs. 23, 46, 56 and 58 the first row of the tangent matrix is given as

$$(S^k_{n+1})_{\text{First Row}} = \begin{bmatrix} \left[\left(\frac{1}{\beta_2 h^2}\right) M_{FF} + \left(\frac{1}{\beta_2 h}\right) C_{FF} + K_{FF}\right] \\ \left[\left(\frac{1}{\gamma_1 h}\right) M_{FB} + C_{FB} - \left[\frac{\partial}{\partial \beta} R_F\right]\right] \\ \left[\frac{\partial}{\partial \zeta} R_F\right] \\ 0 \\ 0 \end{bmatrix}^T \tag{60}$$

where the matrices M_{FF}, C_{FF}, M_{FB}, and C_{FB} are assumed to be constant for the derivation of the tangent matrix.

D. Convergence Criteria

Figure 4 presents the high level flow of the convergence routine. The Newton-Raphson method outlined above works well for the majority of time steps and sub-iteration steps. However, given the large number of states that are being solved, the Newton-Raphson on occasion will not yield a lower norm of the residual vector. If that happens the state correction, Δq is modified using a line search algorithm, such that

$$\Delta q = \alpha\left(-\left[S^k_{n+1}\right]^{-1} r^k_{n+1}\right) \tag{61}$$

Crude bracket values for the scaling parameter α are first found by calculating the residual vector at various values of α such that

$$0 < \alpha_l < \alpha < \alpha_u < 1 \tag{62}$$

The lower and upper bounds (subscripts l and u) on α are then used in a quadratic curve formula[7]

$$\alpha = \frac{1}{2}\left(\frac{\left(\alpha_m^2 - \alpha_u^2\right)\|r_l\| + \left(\alpha_u^2 - \alpha_l^2\right)\|r_m\| + \left(\alpha_l^2 - \alpha_m^2\right)\|r_u\|}{\left(\alpha_m - \alpha_u\right)\|r_l\| + \left(\alpha_u - \alpha_l\right)\|r_m\| + \left(\alpha_l - \alpha_m\right)\|r_u\|}\right) \tag{63}$$

where

$$\alpha_m = \frac{\alpha_u - \alpha_l}{2} \tag{64}$$

and r_m is evaluated at α_m. Equation 63 is iterated upon until a satisfactory convergence on α is reached. The change in the, Δq is then updated in accordance with Eqs. 49, 50, and 61. In almost all cases this line search method provides an excellent update state, Δq.

It is possible however for the Newton-Raphson method to converge to a local minimum of $\|r\|_2$. In this case, the line search scaling parameter, α will be zero. This situation is determined by monitoring the value of α for several sub-iteration steps. If $\alpha < \varepsilon$ for more than a user defined number of sequential sub-iteration steps, than α is arbitrarily set to

$$\alpha = 0.25 + 0.25k_i \tag{65}$$

where k_i is the number of times a local minimum has been reached and ε is a user defined and ≈ 0. The state update, Δq is then computed using Eq. 61. Using this heuristic approach, the Newton-Raphson search is moved away from a local minimum and allowed to continue searching for the global minimum of $\|r\|_2$. In practice this method has shown excellent results at resolving convergence to local minimums.

IV. Numerical Examples

Two different models are presented here to highlight the main characteristics of the proposed method. The first model is a simple cantilevered beam shown in Figure 5 with properties given in Table 1.

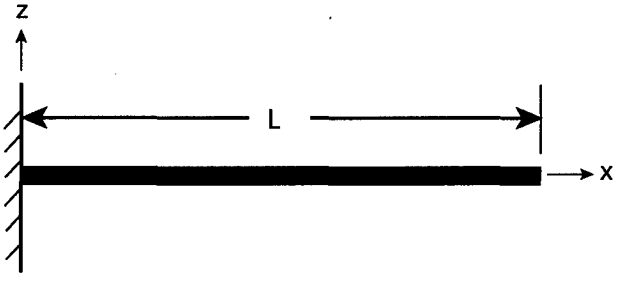

Figure 5. Cantilevered Beam

Three integration techniques were run on the beam model: Matlab's ODE15S, Trapezoidal Method, Modified Generalized-α Method . For the beam model Eq. 23 is solved where the B reference frame states, β, are removed. Linear and nonlinear solutions are presented by either setting M_{ff} and C_{ff} to the initial state or being updated at each time step. A plot of the linear solution with the three integration methods is shown in Figure 6 and a table of the relevant features is presented in Table 2. All three methods are seen to provide similar results. The trapezoidal method and Generalized-α Method both provide a relatively quick solution to the differential equations, while Matlab's ODE15S takes almost 2 orders of magnitude longer due to the stiffness of the equations. For the nonlinear case, Figure 7, Matlab's ODE15S is seen to diverge from the other solutions. This is due to the inability of the Matlab's solvers to handle high accuracy stiff ODEs. Tighter tolerances did move Matlab's ODE15S solution slightly closer to the trapezoidal and Modified Generalized-α Method solutions, but at the risk of early termination or increased integration time of several orders of magnitude. Matlab's other solvers performed in a similar manner. This is not surprising as Matlab's ODE solvers are intended for non-stiff, lower order ODEs. Table 3 provides a comparison of computation time for the various integration methods and cases.

Cantilevered Beam Properties		
Property	Value	Units
Beam Length	1.0	m
$K_{11} = EA$	10^6	N
$K_{22} = GJ$	50	$N \cdot m^2$
$K_{33} = EI_2$	50	$N \cdot m^2$
$K_{44} = EI_3$	10^3	$N \cdot m^2$
Mass per unit length	0.2	$kg \cdot m^{-1}$
I_{11} per unit length	10^{-4}	$kg \cdot m$
I_{22} per unit length	10^{-6}	$kg \cdot m$
I_{33} per unit length	10^{-4}	$kg \cdot m$
Elements in beam	10	—
Number of Second-Order states	40	—

Table 1. Geometric, Stiffness, and Inertia Properties of Cantilevered Beam (only non-zero terms are listed)

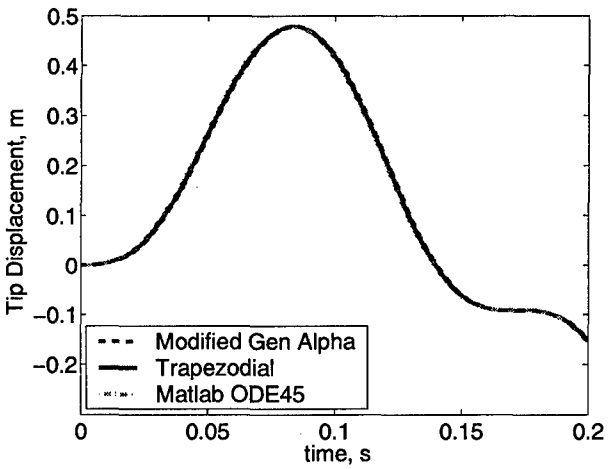

Figure 6. Linear Elastic Solution of Cantilevered Beam with Tip Force Actuation of $10\sin(20t)$

Linear Elastic Solution of Cantilevered Beam, Numerical Results			
Integration Scheme	CPU Time	Maximum Difference	Convergence Parameters
MatlabODE15S	1746.80 s	0	Relative = 10^{-3}, Absolute = 10^{-5}
Trapezoidal	23.64 s	0.0064	NA
Generalized-α Method	28.47 s	0.0124	$\|\|r\|\|_2 = 5 * 10^{-5}$, $\rho_\infty = 0.99$

Table 2. Comparative Results of Various Integration Schemes for a Cantilevered Beam

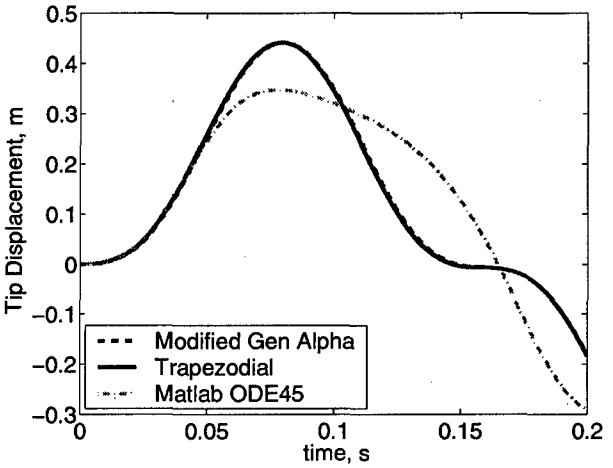

Figure 7. Nonlinear Elastic Solution of Cantilevered Beam with Tip Force Actuation of $10\sin(20t)$

Computational Times for Cantilevered Beam		
Integration Scheme	Linear Solution	Nonlinear Solution
MatlabODE15S	$1746.812s$	$9946.000s$
Trapezoidal	$23.641s$	$38.781s$
Modified Generalized-α Method	$28.469s$	$80.032s$

Table 3. Computational Times for Trapezoidal and Modified Generalized-α Method Integration Schemes for Very Flexible Aircraft

For the next result, the cantilevered beam is pinned at the 50% location as seen in Figure 8. In this case

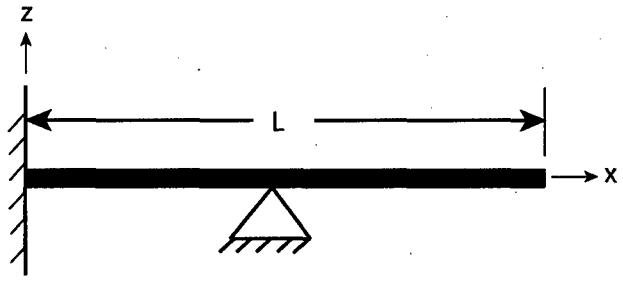

Figure 8. Cantilevered Beam Constrained at Mid Point

the elastic equations of motion, Eq. 23, have been modified by Su and Cesnik[31] and the authors through the stiffness matrix to include algebraic constraint equations with Lagrange Multipliers, λ_L. The augmented system given in Eq. 23 without the B reference frame linear and angular velocities, β,becomes

$$\begin{bmatrix} M_{FF} & 0 \\ 0 & 0 \end{bmatrix} \begin{Bmatrix} \ddot{\epsilon} \\ \ddot{\lambda}_L \end{Bmatrix}_{i+1} = -\begin{bmatrix} C_{FF} & 0 \\ 0 & 0 \end{bmatrix} \begin{Bmatrix} \dot{\epsilon} \\ \dot{\lambda}_L \end{Bmatrix}_{i+1} - \begin{bmatrix} K_{FF} & \Phi^T \\ \Phi & 0 \end{bmatrix} \begin{Bmatrix} \epsilon \\ \lambda_L \end{Bmatrix}_{i+1} + \begin{Bmatrix} R_F \\ \Phi\epsilon_i - (h_i - h_0) \end{Bmatrix} \tag{66}$$

where Φ, contains the constraint relation, λ_L is the Lagrange multiplier, i is a time index, and h_i and h_0 are the displacement information at the current time step i and the initial time step 0. For this case Matlab does not have a solver which can handle differential algebraic equations (DAEs) higher than index 1. Recall the index of a DAE is defined as the number of times which the algebraic equation must be differentiated before a standard ODE form is reached. For the current case the constraint equation (before expressing it in discrete form) is of the form

$$f(\epsilon) = 0 \tag{67}$$

Differentiating $f(\epsilon)$ two times yields

$$0 = \left[\frac{\partial}{\partial\epsilon} f\right] \dot{\epsilon} \tag{68}$$

$$0 = \left[\frac{\partial^2}{\partial\epsilon^2} f\right] \dot{\epsilon} + \left[\frac{\partial}{\partial\epsilon} f\right] \ddot{\epsilon} \tag{69}$$

such that the later is in ODE form. The results for this case with a linear solution are seen in Figure 9. While the trapezoidal case appears to be stable for the linearized solution, a closer examination of some of the discrete eigenvalues of the amplification matrix, Table 4, reveal a slight instability (greater than unity or repeated eigenvalues on the unit circle). The eigenvalues with only real parts and associated eigenvectors are due to the Lagrange multipliers. By examining the unstable elastic eigenvalues it is found that they are also controlled by the Lagrange multipliers. The slight instability is not seen over relatively short periods of integration. This is consistent with the proof of Cardona and Geradin.[8] For the nonlinear solution, Figure 10, it is seen that the trapezoidal method is unstable. This can also be seen from the residual term as shown in Figure 11. Also from Figure 10, the Generalized-α Method maintains long term stability. However due to the high frequency numerical damping of the Modified Generalized-α Method, there is a loss of high frequency content. Solution time is also longer for the Modified Generalized-α Method , Table 5, due to the recursive nature of the sub-iteration scheme until a satisfactory residual term is obtained. The user must trade long term stability with the loss of high frequency content.

For very flexible aircraft repeated eigenvalues on the unit circle can come from the aircraft configuration (joined wing concept),[1] unconstrained rigid body degrees of freedom due to a free flying aircraft, or an aircraft controller. A model based upon Ref. 3 is shown in Figure 1 and relevant physical properties are summarized in Table 6. Here results are presented for a nonlinear flexible simulation where the aircraft is given a square aileron input, Figure 12. Representative solutions of the longitudinal and vertical B reference frame velocities are shown in Figure 13 and pitch and yaw rates in Figure 14 for a trapezoidal and Generalized-α Method integration. While the two methods track resonably well for the first 10 seconds and then the trapezoidal

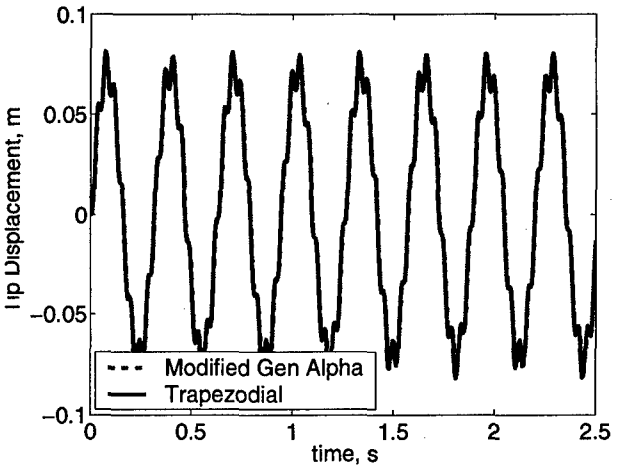

Figure 9. Linear Elastic Solution of Pinned Cantilevered Beam with Tip Force Actuation of $10\sin(20t)$

Eigenvalues due to Lagrange Multiplier Constraints			
Eigenvalue	Real Part	Imaginary Part	State
λ_{75}	-0.999992847	0	Lagrange Multiplier
λ_{78}	-0.999996417	0	Lagrange Multiplier
λ_{81}	-0.999999461	0	Lagrange Multiplier
$\lambda_{76,77}$	-1.000003576	+/- 0.000006194i	Strain
$\lambda_{79,80}$	-1.000001791	+/- 0.000003103i	Strain
$\lambda_{82,83}$	-1.000000269	+/- 0.000000467i	Strain

Table 4. Comparative Results of Various Integration Schemes for a Cantilevered Beam

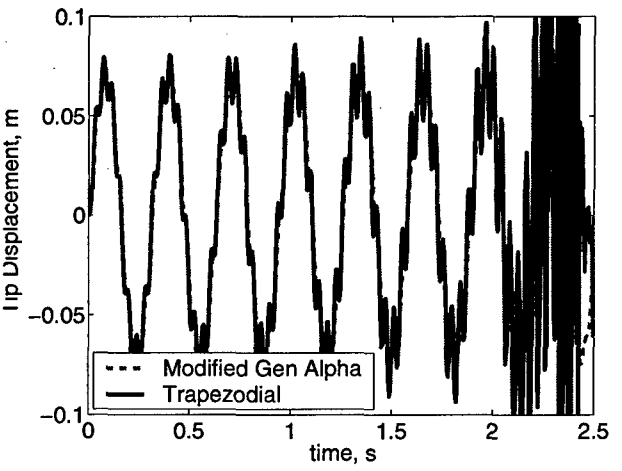

Figure 10. Nonlinear Elastic Solution of Pinned Cantilevered Beam with Tip Force Actuation of $10\sin(20t)$

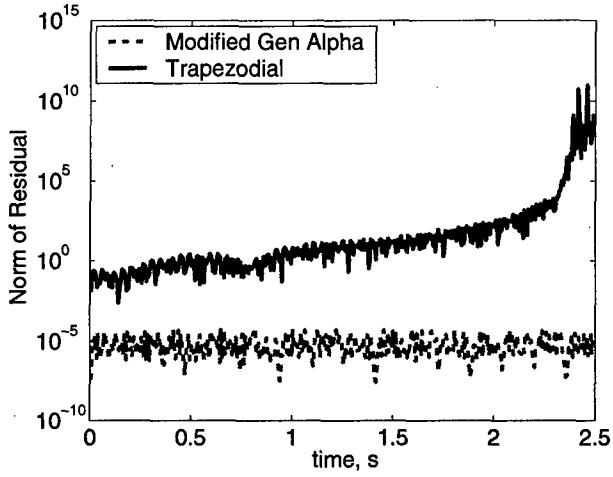

Figure 11. Residual Term, $||r||_2$, of Pinned Cantilevered Beam with Tip Force Actuation of $10\sin(20t)$

Computational Times for Cantilevered Beam		
Integration Scheme	Linear Solution	Nonlinear Solution
Trapezoidal	$73.875s$	$110.531s$
Modified Generalized-α Method	$75.156s$	$258.375s$

Table 5. Computational Times for Trapezoidal and Modified Generalized-α Method Integration Schemes for Very Flexible Aircraft

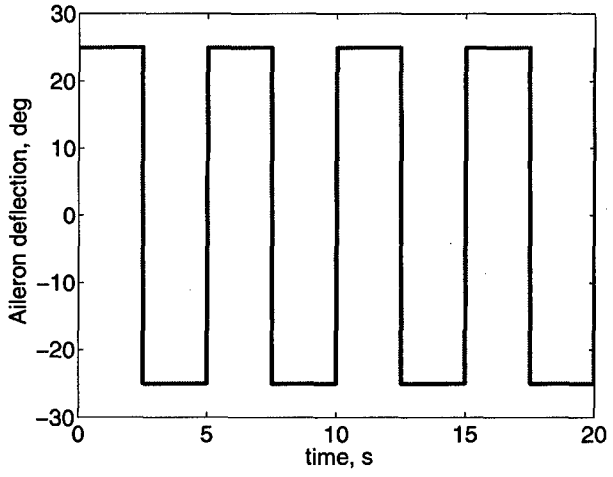

Figure 12. Open Loop Aileron and Rudder Commands

Model Parameters			
Property	Value		Units
	Light	Heavy	
Fuselage Length	26.4		m
Wing Span	58.6		m
Wing Area	196.3		m^2
Root Chord	4.5		m
Tip Chord	2.2		m
Aspect Ratio	17.5		—
Horizontal Tail Span	18.0		m
Horizontal Root Chord	3.5		m
Horizontal Tip Chord	2.45		m
Vertical Tail Span	4.0		m
Vertical Root Chord	2.45		m
Vertical Tip Chord	2.0		m
Wing/Horizontal Tail Airfoil	NACA 4415		—
Vertical Tail Airfoil	NACA 0012		—
Aileron Location	16.3 to 22.8		m
Aileron, Elevator, Rudder Chord	$0.2c_{local}$		
Elevator Location	1.8 to 9.0		m
Rudder Location	0.8 to 3.2		m
Aircraft Angle of Attack	0.64°	6.37°	—
Elevator Deflection Angle	−4.11°	−13.43°	—
Fuel Mass	0	32,000	kg
Total Mass	$1.52 \cdot 10^4$	$4.72 \cdot 10^4$	kg
Fuel Fraction	0.0	67.8	%
I_{xx}^{ss} *	$9.61 \cdot 10^5$	$1.17 \cdot 10^6$	$kg \cdot m^2$
I_{yy}^{ss}	$8.21 \cdot 10^5$	$2.94 \cdot 10^6$	$kg \cdot m^2$
I_{zz}^{ss}	$1.75 \cdot 10^6$	$3.93 \cdot 10^6$	$kg \cdot m^2$
I_{xy}^{ss}	0	0	$kg \cdot m^2$
I_{xz}^{ss}	0	0	$kg \cdot m^2$
I_{yz}^{ss}	$-1.65 \cdot 10^4$	$-4.72 \cdot 10^4$	$kg \cdot m^2$
Elements per wing	9		—
Elements per horizontal tail	5		—
Elements per vertical tail	5		—
Elements in fuselage	10		—
Total Number of Elements	48		—

*Note: I^{ss} are the inertia properties in a steady state configuration

Table 6. Geometric and Inertia Properties of the Flexible Aircraft Model

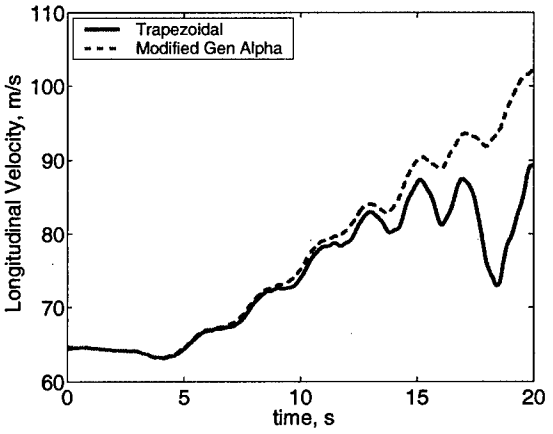

(a) Longitudinal B Reference Frame Velocity

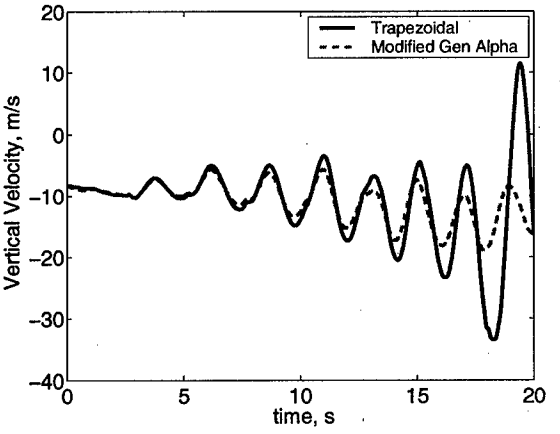

(b) Vertical B Reference Frame Velocity

Figure 13. B Reference Frame Velocities for Trapezoidal and Generalized-α Method Integration

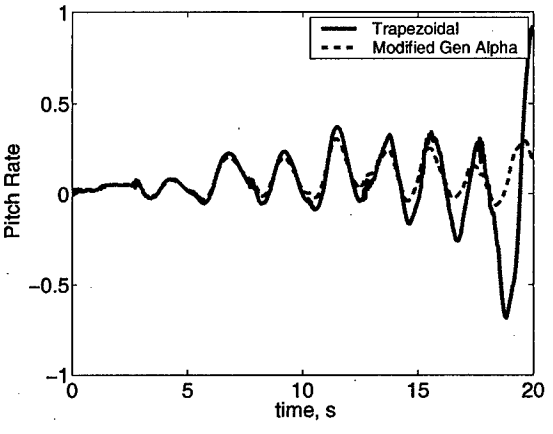

(a) Pitch Rate of B Reference Frame

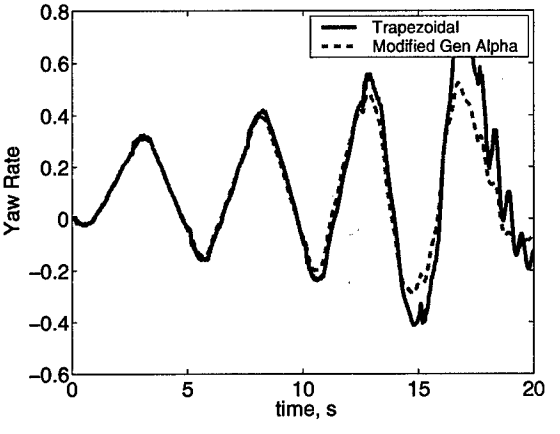

(b) Yaw Rate B Reference Frame

Figure 14. B Reference Frame Velocities for Trapezoidal and Generalized-α Method Integration

method begins to diverge. The divergence can be better seen by examining the two norm of the residual shown in Figure 15, while the Modified Generalized-α Method was commanded to keep the norm below 1.0 (figure not shown). The penalty paid for this long term stability is in computational time as shown in

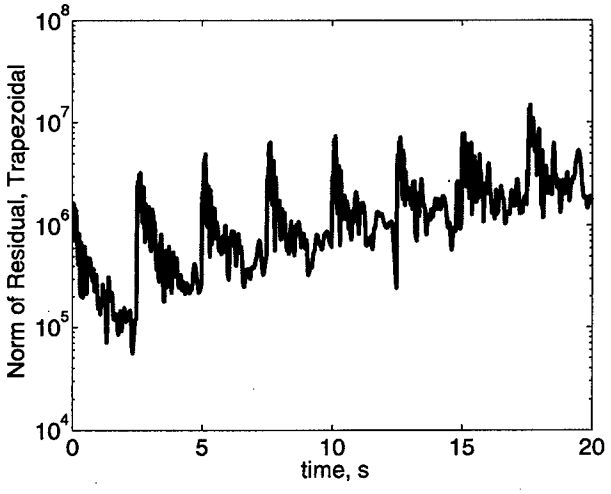

Figure 15. Residual Term, $||r||_2$, of Trapezoidal Integration

Table 7.

Computational Times	
Trapezoidal	3902.8 s
Modified Generalized-α Method	42261.2 s

Table 7. Computational Times for Trapezoidal and Modified Generalized-α Method Integration Schemes for Very Flexible Aircraft

V. Conclusion

The proposed integration method, i.e., the Modified Generalized-α Method, shows good correlation with existing integration schemes for systems which are stiff and have a large number of states. Its main limiting factors are an increase in computational time over simpler first order methods and the attenuation of high frequency data due to the dissipative nature of the integration scheme. It was also shown that the method handles DAE of index higher than 1 and preserves long term stability when solving nonlinear elastic EOM.

NASA Acknowledgement?

References

[1]Tilmann, C. P., Flick, P. M., Martin, C. A., and Love, M. H., "High-Altitude Long Endurance Technologies for Sensor-Craft," *RTO AVT Symposium on "Novel Vehicle Concepts and Emerging Vehicle Technologies"*, Brussels, Belgium, April 7–10 2003, MP-104-P-26-1.

[2]Whitson, S., "The Proteus, Giving Shape to Forms Unknown," *Private Pilot*, Vol. 33, No. 12, December 1998, pp. 44–50.

[3]Shearer, C. M. and Cesnik, C. E. S., "Nonlinear Flight Dynamics of Very Flexible Aircraft," *AIAA Atmospheric Flight Mechanics Conference and Exhibit*, AIAA, San Fransisco, CA, August 15 - 18 2005, AIAA Paper No. 2005-5805.

[4]Chung, J. and Hulbert, G. M., "A Time Integration Algorithm for Structural Dynamics With Improved Numerical Dissipation: The Generalized-α Method," *Journal of Applied Mechanics*, Vol. 60, June 1993, pp. 371–375.

[5]Jansen, K. E., Whiting, C. H., and Hulbert, G. M., "A Generalized-α Method for Integrating the Filtered Navier-Stokes Equations with a Stabilized Finite Element Method," *Computer Methods in Applied Mechanics and Engineering*, Vol. 190, No. 3-4, 27 October 2000, pp. 305–319.

[6]Peters, D. A. and Cao, W., "Finite State Induced Flow Models Part I: Two-Dimensional Thin Airfoil," *Journal of Aircraft*, Vol. 32, No. 2, March-April 1995, pp. 313–322.

[7]Peters, D. and Johnson, M. J., "Finite-State Airloads for Deformable Airfoils on Fixed and Rotating Wings," *Aeroelasticity and Fluid/Structure Interation, Proceedings of the Winter Annual Meeting*, ASME, November 6–11 1994.

[8]Cardona, A. and Geradin, M., "Time Integration of the Equations of Motion in Mechanism Analysis," *Fix and Structures*, Vol. 33, No. 3, 1989, pp. 801–820.

[9]Bauchau, O. A. and Theron, N. J., "Energy Decaying Scheme for Nonlinear Beam Models," *Computer Methods in Applied Mechanics and Engineering*, Vol. 134, 1996, pp. 37–56.

[10]Stevens, B. L. and Lewis, F. L., *Aircraft Control and Simulation*, John Wiley & Sons, Inc., New York, 1992.

[11]Newmark, N. M., "A Method of Computation for Structural Dynamics," *Journal of the Engineering Mechanics Division Proceedings of the American Society of Civil Engineers*, Vol. 85, No. EM 3, July 1959, pp. 67–94, Paper 2094.

[12]Hilber, H. M., Hughes, T. J. R., and Taylor, R. L., "Improved Numerical Dissipation for Time Integration Algorithms in Stuctural Dynamics," *Earthquake Engineering and Structural Dynamics*, Vol. 5, 1977, pp. 283–292.

[13]Fung, T. C., "Numerical dissipation in time-step integration algorithms for structural dynamic analysis," *Prog. Struct. Engng Mater.*, Vol. 5, 2003, pp. 167–180.

[14]Simo, J. C. and Tarnow, N., "The discrete energy-momentum method. Conserving algorithms for nonlinear elastodynamics," *Zeitschift für angewandte Mathematik und Physik (ZAMP), Journal of Applied Mathematics and Physics*, Vol. 43, 1992, pp. 757–792.

[15]Bauchau, O. A., Damilano, G., and Theron, N. J., "Numerical Integration of Non-Linear Elastic Multi-Body Systems," *International Journal for Numerical Methods in Engineering*, Vol. 38, 1995.

[16]Bauchau, O. A. and Theron, N. J., "Energy Decaying Scheme for Nonlinear Elastic Multi-body Systems," *Computers and Structures*, Vol. 59, 1996, pp. 317–331.

[17]Bauchau, O. A., "Computational Schemes for Flexible, Nonlinear Multi-Body Systems," *Multibody System Dynamics*, Vol. 2, 1998, pp. 169–225.

[18]Zhou, X. and Tamma, K. K., "Design, Analysis, and Synthesis of Generalized Single Step Single Solve and Optimal Algorithms for Structural Dynamics," *International Journal for Numerical Methods in Engineering*, Vol. 59, 2004, pp. 597–668.

[19]Kane, T. R. and Levinson, D. A., "A Method for Testing Numerical Integrations of Equations of Motion of Mechanical Systems," *Journal of Applied Mechanics*, Vol. 55, September 1988, pp. 711–715.

[20]Kane, T. R. and Levinson, D. A., "Testing Numerical Integration of Equations of Motion," *Journal of Applied Mechanics*, Vol. 57, March 1990, pp. 248–249.

[21]Souchet, R., "A New Expression of the Energy Theorem in Discrete Mechanical Systems," *Journal of Applied Mechanics*, Vol. 58, December 1991, pp. 1086–1088.

[22]Panda, B., "A Robust Direct-Integration Method for Rotorcraft Maneuver and Periodic Response," *Journal of the American Helicopter Society*, Vol. 37, No. 3, July 1992, pp. 83–85.

[23]Drela, M., "Integrated Simulation Model for Preliminary Aerodynamic, Structural, and Control-Law Design of Aircraft," *40th AIAA/ASME/ASCE/AHS/ASC Structures, Structural Dynamics, and Materials Conference and Exhibit*, St. Louis, Missouri, April 12–15 1999, pp. 1644–1656, AIAA Paper No. 99-1394.

[24]Tang, D. and Dowell, E. H., "Experimental and Theoretical Study on Aeroelastic Response of High-Aspect-Ratio Wings," *Journal of Aircraft*, Vol. 39, No. 8, August 2001, pp. 1430–1441.

[25]Tang, D. and Dowell, E. H., "Experimental and Theoretical Study of Gust Response for High-Aspect-Ratio Wing," *Journal of Aircraft*, Vol. 40, No. 3, March 2002, pp. 419–429.

[26]Patil, M. J., Hodges, D. H., and Cesnik, C. E. S., "Nonlinear Aeroelastic Anaylsis of Complete Aircraft in Subsonic Flow," *Journal of Aircraft*, Vol. 37, No. 5, September-October 2000, pp. 753–760.

[27]Patil, M. J., Hodges, D. H., and Cesnik, C. E. S., "Nonlinear Aeroelasticity and Flight Dynamics of High-Altitude Long-Endurance Aircraft," *Journal of Aircraft*, Vol. 38, No. 1, January-February 2001, pp. 95–103, Presented as Paper AIAA 99-1470.

[28]Brown, E. L., *Integrated Strain Actuation in Aircraft with Highly Flexible Composite Wings*, Ph.D. thesis, Massachusetts Institute of Technology, Boston, Massachusetts, June 2003, PhD Thesis.

[29]Cesnik, C. E. S. and Brown, E. L., "Modeling of High Aspect Ratio Active Flexible Wings for Roll Control," *Proceedings of the 43rd AIAA/ASME/ASCE/AHS Structures, Structural Dynamics, and Materials Conferences*, Denver, Colorado, April 22–25 2002, AIAA Paper No. 2002-1719.

[30]Geradin, M. and Rixen, D., *Mechanical Vibrations: Theory and Applications to Structural Dynamics*, John Wiley and Sons Ltd., 2nd ed., May 1997.

[31]Su, W. and Cesnik, C. E. S., "Aeroelastic Response of Highly Flexible Flying Wings," *47th AIAA/ASME/ASCE/AHS/ASC Structures, Structural Dynamics, and Materials Conference and Exhibit*, Newport, RI, May 1–4 2006, AIAA Paper No. 2006-1636.

[32]Kreyszig, E., *Advanced Engineering Mathematics*, John Wiley & Sons, Inc., New York, 7th ed., 1993.

[33]Reid, J. G., *Linear System Fundamentals Continuous and Discrete, Classic and Modern*, McGraw-Hill, Inc., New York, 1983.